

Special Section:

Atmospheric PM_{2.5} in China: physics, chemistry, measurements, and modeling

Key Points:

- NO₃ radical chemistry was dominant in nitrate production in the polluted atmosphere in Hangzhou
- The isotopic fractionation effect in the NO_{x(g)}-NO_{3⁻(p) conversion showed a greater impact on the source apportionment of nitrate aerosols}
- Coal combustion was the main source of nitrate aerosols in Hangzhou

Supporting Information:

Supporting Information may be found in the online version of this article.

Correspondence to:

Y.-L. Zhang,
zhangyanlin@nuist.edu.cn;
dryanlinzhang@outlook.com

Citation:

Fan, M.-Y., Zhang, W., Zhang, Y.-L., Li, J., Fang, H., Cao, F., et al. (2023). Formation mechanisms and source apportionments of nitrate aerosols in a megacity of eastern China based on multiple isotope observations. *Journal of Geophysical Research: Atmospheres*, 128, e2022JD038129. <https://doi.org/10.1029/2022JD038129>

Received 6 NOV 2022

Accepted 23 FEB 2023

Author Contributions:

Conceptualization: Yan-Lin Zhang
Formal analysis: Mei-Yi Fan
Funding acquisition: Yan-Lin Zhang
Investigation: Mei-Yi Fan
Methodology: Wenqi Zhang, Jianghanyang Li, Huan Fang, Ming Yan, Greg Michalski
Supervision: Yan-Lin Zhang
Writing – original draft: Mei-Yi Fan, Wenqi Zhang
Writing – review & editing: Mei-Yi Fan, Yan-Lin Zhang, Jianghanyang Li, Huan Fang, Fang Cao, Hai Guo, Greg Michalski

© 2023. American Geophysical Union.
All Rights Reserved.

Formation Mechanisms and Source Apportionments of Nitrate Aerosols in a Megacity of Eastern China Based On Multiple Isotope Observations

Mei-Yi Fan^{1,2,3,4} , Wenqi Zhang^{2,3} , Yan-Lin Zhang^{2,3} , Jianghanyang Li^{5,6} , Huan Fang^{5,6} , Fang Cao^{2,3} , Ming Yan⁷ , Yihang Hong³ , Hai Guo⁴, and Greg Michalski^{5,6} 

¹School of Environmental Science and Engineering, Nanjing University of Information Science and Technology, Nanjing, China, ²Atmospheric Environment Center, Joint International Research Laboratory of Climate and Environmental Change (ILCEC), Nanjing University of Information Science and Technology, Nanjing, China, ³School of Applied Meteorology, Nanjing University of Information Science and Technology, Nanjing, China, ⁴Air Quality Studies, Department of Civil and Environmental Engineering, The Hong Kong Polytechnic University, Hong Kong, China, ⁵Department of Earth, Atmospheric, and Planetary Sciences, Purdue University, West Lafayette, IN, USA, ⁶Department of Chemistry, Purdue University, West Lafayette, IN, USA, ⁷College of Artificial Intelligence, Hangzhou Dianzi University, Xiasha Higher Education Zone, Hangzhou, China

Abstract Inorganic nitrate (NO₃⁻) is a crucial component of fine particulate matter (PM_{2.5}) in haze events in China. Understanding the formation mechanisms of nitrate and the sources of NO_x was critical to control the air pollution. In this study, measurements of multiple isotope compositions of nitrate (δ¹⁸O-NO₃⁻, δ¹⁷O-NO₃⁻, and δ¹⁵N-NO₃⁻) in PM_{2.5} were conducted in Hangzhou from 9 October 2015 to 24 August 2016. Our results showed that oxygen anomaly of nitrate (Δ¹⁷O-NO₃⁻: 20.0‰–37.9‰) and nitrogen isotope of nitrate (δ¹⁵N-NO₃⁻: –2.9‰ to 18.1‰) values were higher in winter and lower in summer. Based on Δ¹⁷O-NO₃⁻ observation and a Bayesian model, NO₃ radical chemistry was found to dominate the nitrate formation in winter, while photochemical reaction (NO₂ + OH) was the main pathway in summer. After considering the nitrogen isotopic fractionation in the NO_{x(g)}-NO_{3⁻(p) conversion, the average contributions of coal combustion, vehicle exhausts, biomass burning, and soil emission were 50% ± 9%, 19% ± 12%, 26% ± 15%, and 5% ± 4%, respectively, to nitrate aerosols during the whole sampling period. Coal combustion was the most important nitrate source in Hangzhou, especially in winter (~56%). The contribution of soil emission increased significantly in summer due to active soil microbial processes under high temperature environment.}

Plain Language Summary Inorganic nitrate is a crucial component of fine particulate matter in haze events in China. Understanding the formation mechanisms and sources of nitrate was critical to control the air pollution. In this study, measurements of multiple isotope compositions of nitrate showed that oxygen anomaly and nitrogen isotope of nitrate are distinct in winter and summer. Then, nitrate radical chemistry was found to dominate the nitrate formation in winter, while photochemical reaction (nitrogen dioxide with hydroxyl radical) was the main pathway in summer. After considering the nitrogen isotopic fractionation in the conversion from nitrogen oxides to nitrate particle, coal combustion was the most important nitrate source in Hangzhou, especially in winter (56%) and the contribution of soil emission increased significantly in summer under high temperature environment.

1. Introduction

Atmospheric inorganic nitrate (NO₃⁻) and its precursor NO_x (=NO + NO₂) play crucial roles in haze formation in China (R.-J. Huang et al., 2014; H. Li et al., 2018). Due to limited development of flue gas denitrification technology compared with desulfurization technology (Gao et al., 2018), excess emissions of NO_x have become the most severe pollutant gas in China over the past decade (Zheng et al., 2018). Recently, nitrate has contributed a higher fraction in PM_{2.5} in haze events than in previous observations (Fan et al., 2019; Sun et al., 2015). Nitrogen chemistry is also important in atmospheric chemical processes, since it is involved in the formation of oxidants (e.g., ozone [O₃] and hydroxyl radicals [OH]), which control the atmosphere's self-cleansing capacity (Lu et al., 2019). Thus, the study of NO_x emissions and the nitrate formation mechanism is critical in investigating the formation of haze pollution.

Based on the global NO_x emission inventories, fossil fuel combustion, biomass burning (BB), and agricultural activities are generally considered to be the dominant sources of tropospheric NO_x (Jaeglé et al., 2005; Martin et al., 2003). However, NO_x emission assessments conducted through satellite-based studies and emission inventory methods usually cause misclassification of various sources, especially in urban areas. Stable isotope methodology has shown significant advantages in recognizing different NO_x sources since the $\delta^{15}\text{N}$ signatures are unique in various sources (Elliott et al., 2019). For instance, the $\delta^{15}\text{N}$ of NO_x emitted from combustion processes, such as BB ($1.8\text{‰} \pm 4.1\text{‰}$) and fossil fuel combustion (0‰ – 20‰), have higher values comparing to other NO_x emission sources (Elliott et al., 2009; Fibiger & Hastings, 2016). NO_x is depleted in ^{15}N when derived from natural sources such as nitrification/denitrification in soil ($< -20\text{‰}$; Felix & Elliott, 2014; D. Li & Wang, 2008; D. J. Miller et al., 2018; Su et al., 2020; Z. Yu & Elliott, 2017). However, nitrogen isotopic composition of nitrate is also depended on the nitrogen isotopic fractionation ($\Delta^{15}\text{N}$) during the oxidation of NO_x into atmospheric nitrate besides to the sources of NO_x (Elliott et al., 2007; Vicars et al., 2013). Studies that considered the isotopic fractionation only focused on the equilibrium isotopic effect (EIE) in the NO_x - HNO_3 conversion, the kinetic isotopic effect (KIE) and the photochemical isotopic fractionation effect (PHIFE) in NO_x cycle were neglected in the calculation of $\Delta^{15}\text{N}$ and the NO_x source apportionment (J. Li et al., 2020). The nitrogen isotopic fractionation occurred in every step of NO_x oxidation (Z. Li et al., 2019). Fang et al. (2021) pointed that ^{15}N are more enriched in nitrate produced through N_2O_5 hydrolysis, whereas the $\text{NO}_2 + \text{OH}$ pathway produces nitrate with lower $\delta^{15}\text{N}$ values.

The transformation of NO_x to NO_3^- is a combination of the NO_x cycle and the nitrate production processes (Text S1 in Supporting Information S1). Briefly, nitrate production involves homogeneous reactions (e.g., $\text{NO}_2 + \text{OH}$ and $\text{NO}_3 + \text{HC}$) and heterogeneous reactions (e.g., the hydrolysis of NO_3 and N_2O_5) in urban areas. The oxidation of NO_2 by OH radicals occurs during the day with sunlight. The reactions involving NO_3 radicals mainly take place at night, since NO_3 radical can easily be photolyzed. Oxygen isotope ($\delta^{18}\text{O}$ and $\Delta^{17}\text{O}$) analysis of atmospheric nitrate is a powerful technique used to identify nitrate formation pathways (Alexander et al., 2009, 2020; Michalski et al., 2003; Zong et al., 2020). However, the $\delta^{18}\text{O}$ of NO_3^- ($\delta^{18}\text{O}-\text{NO}_3^-$) was affected by multiple factors, such as nitrate formation pathways, the variation of air temperature, atmospheric pressure, and isotopes of various atmospheric compounds (Elliott et al., 2009; Michalski et al., 2012; Walters & Michalski, 2016). Previous cases showed that the analysis of nitrate production using $\delta^{18}\text{O}-\text{NO}_3^-$ was based on many assumptions, resulting in large uncertainties (Fan et al., 2020; Zong et al., 2020). Unlike $\delta^{18}\text{O}-\text{NO}_3^-$, the observation of $\Delta^{17}\text{O}$ of NO_3^- ($\Delta^{17}\text{O}-\text{NO}_3^-$) has the advantage of nitrate production calculation, making it more convenient and accurate. Its principle is that the only exception to the mass-dependent oxygen isotopic fractionation rule ($\delta^{17}\text{O} = 0.52 \times \delta^{18}\text{O}$) occurs during O_3 production (Thiemens, 1999). This isotopic fractionation that appears independent of relative mass differences is termed as mass-independent fractionation and is quantified by $\Delta^{17}\text{O} = \delta^{17}\text{O} - 0.52 \times \delta^{18}\text{O}$ (Thiemens, 1999). The positive $\Delta^{17}\text{O}-\text{NO}_3^-$ value is due to the transfer of O atoms from O_3 (Alexander et al., 2009). Thus, the $\Delta^{17}\text{O}-\text{NO}_3^-$ can directly reflect the different contributions of O_3 oxidation in various nitrate formation pathways. In recent years, the use of $\Delta^{17}\text{O}-\text{NO}_3^-$ has got considerable attention in revealing nitrogen chemistry in China. For instance, nocturnal chemistry was found to contribute equally with $\text{NO}_2 + \text{OH}/\text{H}_2\text{O}$ to nitrate formation near ground surface but dominate the production of nitrate at high altitude (~ 260 m) in winter (Fan et al., 2021). The hydrolysis of N_2O_5 was found to be an important mechanism of nitrate formation over the Himalayan–Tibetan Plateau (Lin et al., 2021).

Yangtze River Delta (YRD) region, as one of the most economically developed zones in China, is experiencing serious and complex air pollution problems due to the high energy consumption and the rapid growth of vehicles (Ming et al., 2017). Hangzhou is one of the largest cities in the YRD, which is a typical megacity with huge energy consumption and rapid growth in population and vehicles (Q. Zhang et al., 2008). However, long-term observations of nitrate isotopes are still lack in the YRD, which are necessary for exploring the formation mechanisms of nitrate and the sources of NO_x in different seasons and provide effective scientific basis for the government to develop emission reduction strategies under different emission backgrounds. Previously, field measurements have showed obvious seasonal variations in meteorology, tracer gases, and particulate pollutants in urban regions (Chen et al., 2020; K. Zhang et al., 2020; Y.-L. Zhang & Cao, 2015). Highest levels of $\text{PM}_{2.5}$ and its major chemical components (e.g., organic carbon and secondary ions) were normally observed in the cold seasons in the YRD (Feng et al., 2006; Ming et al., 2017). Clear seasonal trends for CO , SO_2 , and NO_2 were observed with the maximum concentrations in winter and the minimum in summer, while O_3 exhibited an opposite trend (Ding et al., 2013; H. Zhang et al., 2015). Besides, previous studies found that the concentrations of OH,

HO₂, and NO₃ radicals were generally much lower in winter than those in summer (Asaf et al., 2010; Rohrer & Berresheim, 2006; Tan et al., 2018; Walker et al., 2015; H. Wang et al., 2017). These results implied that the NO_x emission sources and chemical mechanisms producing nitrate aerosols might be different in different seasons, while the nitrate formation mechanisms and sources of NO_x remain unclear in the YRD region.

In this study, field measurements of multiple isotopes in nitrate aerosols ($\delta^{15}\text{N-NO}_3^-$, $\delta^{17}\text{O-NO}_3^-$, and $\delta^{18}\text{O-NO}_3^-$) were conducted from 2015 to 2016 in Hangzhou, a megacity in the YRD. The relative importance of each nitrate formation pathway in Hangzhou was calculated using the observation of oxygen isotopic compositions. The seasonal variations of nitrate formation mechanisms and the possible factors were analyzed. The nitrogen isotopic fractionation was calculated based on the contribution of each nitrate formation pathway and then $\delta^{15}\text{N-NO}_x$ was obtained accordingly. The values of $\delta^{15}\text{N-NO}_x$ were applied in the nitrate source apportionment in Hangzhou using a Bayesian model.

2. Materials and Methods

2.1. Sampling Site and Atmospheric Observations

PM_{2.5} sample collection was conducted from 9 October 2015 to 24 August 2016, in Hangzhou (Figure S1 in Supporting Information S1). The aerosol sampling site was located at the top of Zhouyiqing building (about 25 m above the ground) in the campus of Zhejiang University (30.23°N, 120.17°E), 500 m from a busy traffic road (Yugu Road), and 400 m from the largest area covered with vegetation in Hangzhou city (Hangzhou Botanical Garden and scenic area of the West Lake). Aerosol samples were collected on precombusted quartz-fiber filters for 23.5 hr every week using a high-volume aerosol sampler (KC100, Qingdao, China) at a flow rate of 1 m³ min⁻¹. After sampling, all filters were wrapped in aluminum foil, sealed in air-tight polyethylene bags, and stored at -26°C for later analysis. A field blank was obtained by placing the blank filter on the filter holder for 10 min without sampling. The synchronized observation of the PM_{2.5} concentrations and the pollutant gases (e.g., NO₂, O₃, SO₂, and CO) was conducted at the Wolongqiao Environmental Supervising Station (about 4 km from the sampling site). Meteorological data were from the meteorological observation station in Hangzhou (3 km from the sampling site).

2.2. Chemical Analysis

The concentrations of inorganic ions (including NO₃⁻, SO₄²⁻, NH₄⁺, Cl⁻, K⁺, Ca²⁺, and Na⁺) were detected with an ion chromatography instrument (ICS 5000+, Thermo Fisher Scientific, USA). After sampling, one 2.54 cm² piece of the sampled filter was extracted with 15 mL of Milli-Q water (18.2 Ω) for 30 min. The recovery of each ion was in the range of 90%–110%, and the precision was less than 2%. The method detection limit of NO₃⁻, a target species, was 0.08 ng m⁻³. The details of this method can be found elsewhere (Fan et al., 2019).

Nitrogen and oxygen isotopic compositions ($\delta^{15}\text{N}$, $\delta^{17}\text{O}$, and $\delta^{18}\text{O}$) of NO₃⁻ in the sampled filters were measured after conversion of NO₃⁻ to nitrous oxide (N₂O) by optimized bacterial denitrification process (H. Yu et al., 2021; Zhao et al., 2019). Briefly, a small piece of the sampled filter (at least containing 0.8 μgN) was extracted with 5 mL Milli-Q water for 30 min. After extraction, the solution was then filtered by a membrane filter (0.22 μm) to remove the insoluble particles and was prepared to proceed chemical conversion procedure. In the conversion process for oxygen isotopes, NO₃⁻ was initially transformed to N₂O by denitrifying bacteria (ATCC13985, *Pseudomonas chlororaphis*). Subsequently, N₂O was decomposed into N₂ and O₂ by carrying out in a platinum tube at 650°C. The produced N₂ and O₂ was then analyzed $\delta^{15}\text{N}$, $\delta^{17}\text{O}$, and $\delta^{18}\text{O}$ by an isotope ratio mass spectrometer (MAT253, Thermo Fisher Scientific, USA), and $\Delta^{17}\text{O}$ ($=\delta^{17}\text{O} - 0.52 \times \delta^{18}\text{O}$) was then calculated. The analytical accuracies of $\delta^{15}\text{N}$, $\delta^{18}\text{O}$, and $\Delta^{17}\text{O}$ were 0.08‰, 0.24‰, and 0.04‰, respectively. Detailed methods are described in H. Yu et al. (2021) and Zhao et al. (2019).

2.3. Calculation Method of Nitrate Formation Pathways

In this work, $\Delta^{17}\text{O-NO}_3^-$ was used to identify nitrate formation pathways and three formation pathways (P1: NO₂ + OH, P2: NO₃ + HC/H₂O, and P3: N₂O₅ + H₂O) were considered as the potential formation mechanisms of nitrate aerosols. Based on isotope mass balance, the observed $\Delta^{17}\text{O-NO}_3^-$ values can be expressed as (Alexander et al., 2009)

$$\Delta^{17}\text{O-NO}_3^- = \Delta^{17}\text{O-HNO}_3(\text{P1}) \times f_{\text{P1}} + \Delta^{17}\text{O-HNO}_3(\text{P2}) \times f_{\text{P2}} + \Delta^{17}\text{O-HNO}_3(\text{P3}) \times f_{\text{P3}} \quad (1)$$

where $\Delta^{17}\text{O-HNO}_3(\text{P1})$, $\Delta^{17}\text{O-HNO}_3(\text{P2})$, and $\Delta^{17}\text{O-HNO}_3(\text{P3})$ represent the $\Delta^{17}\text{O}$ values of HNO_3 produced by the three pathways, respectively. f_{P1} , f_{P2} , and f_{P3} are the proportions of P1, P2, and P3 to nitrate production and $f_{\text{P1}} + f_{\text{P2}} + f_{\text{P3}} = 1$. The $\Delta^{17}\text{O-HNO}_3$ in each nitrate formation pathway can be calculated by $\Delta^{17}\text{O}$ of tropospheric O_3 ($\Delta^{17}\text{O-O}_3$) and α (a notation of the fraction of NO_2 oxidized from O_3 ; Alexander et al., 2009):

$$\Delta^{17}\text{O-HNO}_3(\text{P1})(\text{‰}) = 2/3\alpha \times \Delta^{17}\text{O-O}_3^* \quad (2)$$

$$\Delta^{17}\text{O-HNO}_3(\text{P2})(\text{‰}) = 2/3\alpha \times \Delta^{17}\text{O-O}_3^* + 1/3\Delta^{17}\text{O-O}_3^* \quad (3)$$

$$\Delta^{17}\text{O-HNO}_3(\text{P3})(\text{‰}) = 2/3\alpha \times \Delta^{17}\text{O-O}_3^* + 1/6\Delta^{17}\text{O-O}_3^* \quad (4)$$

where $\Delta^{17}\text{O-O}_3^*$ ($=1.5 \times \Delta^{17}\text{O-O}_3$) value was $\sim 39\text{‰}$ based on the previous observations of $\Delta^{17}\text{O-O}_3$ ($\sim 26\text{‰}$; Ishino et al., 2017; Vicars & Savarino, 2014). The α values were estimated by an i_{N} RACM model (Text S2 and Figure S2 in Supporting Information S1) and varied from 0.71 to 0.99 (Figure S3 in Supporting Information S1), indicating that the oxidation of NO in NO_x cycle was dominated by O_3 . This result was similar to those previously calculated in Beijing (0.66–0.96; Y. L. Wang et al., 2019) and Shanghai (0.86–0.96; He et al., 2020). Using the α , the endmembers of $\Delta^{17}\text{O-HNO}_3(\text{P1})$, $\Delta^{17}\text{O-HNO}_3(\text{P2})$, and $\Delta^{17}\text{O-HNO}_3(\text{P3})$ were calculated as 18.4‰–25.6‰, 31.4‰–38.6‰, and 24.9‰–32.1‰ (Figure S3 in Supporting Information S1). Then, the relative contribution of each pathway in Equation 1 can be assessed with a Bayesian model (Text S3 in Supporting Information S1).

2.4. Calculation Method of Nitrogen Isotopic Fractionation Effects

The discrepancy of $\delta^{15}\text{N}$ between $\text{NO}_{x(\text{g})}$ and NO_3^- (nitrogen isotopic fractionation effects, $\Delta^{15}\text{N}$) can be expressed as (J. Li et al., 2020; Walters & Michalski, 2016):

$$\Delta^{15}\text{N} = \Delta^{15}\text{N}_1 + \Delta^{15}\text{N}_2 \quad (5)$$

where $\Delta^{15}\text{N}_1$ and $\Delta^{15}\text{N}_2$ are the nitrogen isotopic fractionations occur in the $\text{NO}_{x(\text{g})}$ cycle and $\text{NO}_{2(\text{g})}\text{-HNO}_{3(\text{g})}$ conversion, respectively. According to a recent study of isotopic fractionation between NO and NO_2 using an atmospheric simulation chamber at atmospheric relevant NO_x levels, isotopic fractionation in the NO_x cycle can be obtained by the following equation (J. Li et al., 2020):

$$\epsilon_{\text{NO}_2} = \delta^{15}\text{NO}_2 - \delta^{15}\text{NO}_x = \frac{(\alpha_2 - \alpha_1) \times A + \left(\alpha^{15} \left(\frac{\text{NO}_2}{\text{NO}} \right) - 1 \right)}{A + 1} \times (1 - f(\text{NO}_2)) \times 1,000\text{‰} \quad (6)$$

where $(\alpha_2 - \alpha_1)$ is the fractionation factor of the Leighton cycle isotope effect, a combination of KIE and PHIFE and was 0.990 ± 0.005 (J. Li et al., 2020). $\alpha^{15}(\text{NO}_2/\text{NO})$ factor represents EIE between NO and NO_2 which was tested to be 1.0275 ± 0.0012 . $f(\text{NO}_2)$ in this equation is the fraction of NO_2 in NO_x and A represents the NO_2 lifetime (calculation of A is described in Text S4 and Figure S4 in Supporting Information S1).

As for the subsequent of $\text{NO}_2\text{-HNO}_3$ conversion, the equilibrium isotope effect between NO_2 and NO_3 (NO_2 and N_2O_5) can be calculated as (Walters & Michalski, 2016)

$$\epsilon_{\text{NO}_3} = 1,000 \times ({}^{15}\alpha_{\text{NO}_3/\text{NO}_2} - 1) \quad (7)$$

$$\epsilon_{\text{N}_2\text{O}_5} = 1,000 \times ({}^{15}\alpha_{\text{N}_2\text{O}_5/\text{NO}_2} - 1) \quad (8)$$

where ϵ_{NO_3} and $\epsilon_{\text{N}_2\text{O}_5}$ represent the isotopic fractionation factor in $\text{NO}_2\text{-NO}_3$ equilibrium and $\text{NO}_2\text{-N}_2\text{O}_5$ equilibrium, respectively. ${}^{15}\alpha_{X/Y}$ is the nitrogen equilibrium isotopic fractionation factor between X and Y , which can be obtained by (Walters & Michalski, 2016)

$$1,000 \times ({}^{15}\alpha_{X/Y} - 1) = \frac{A}{T^4} \times 10^{10} + \frac{B}{T^3} \times 10^8 + \frac{C}{T^2} \times 10^6 + \frac{D}{T} \times 10^4 \quad (9)$$

where T is the air temperature (K) and A , B , C , and D are constants (Table S1 in Supporting Information S1). In this way, ϵ_{NO_2} , ϵ_{NO_3} , and $\epsilon_{\text{N}_2\text{O}_5}$ can be calculated, and then the $\Delta^{15}\text{N}_1$ and $\Delta^{15}\text{N}_2$ can be further calculated by the isotopic fractionation factor (ϵ_{NO_2} , ϵ_{NO_3} , and $\epsilon_{\text{N}_2\text{O}_5}$) and the contribution of each formation pathway:

$$\Delta^{15}\text{N}_1 = \epsilon_{\text{NO}_2} \times f_{\text{OH}} \quad (10)$$

$$\Delta^{15}\text{N}_2 = \epsilon_{\text{NO}_3} \times f_{\text{NO}_3} + \epsilon_{\text{N}_2\text{O}_5} \times f_{\text{N}_2\text{O}_5} \quad (11)$$

where f_{OH} , f_{NO_3} , and $f_{\text{N}_2\text{O}_5}$ are the contributions of P1 (f_{P1}), P2 (f_{P2}), and P3 (f_{P3}), respectively, which were estimated in Section 2.3. Based on Equations 5–11, the nitrogen isotopic fractionation in $\text{NO}_{x(\text{g})}$ - NO_3^- (p) conversion ($\Delta^{15}\text{N}$) was calculated.

3. Results

3.1. Seasonal Variations in Meteorological Conditions, Trace Gases, and Nitrate Isotopes

According to the report of the meteorological bureau in 2015–2016, four seasons in Hangzhou were divided as autumn (9 October to 30 November 2015), winter (1 December 2015 to 28 February 2016), spring (1 March to 30 May 2016), and summer (1 June to 24 August 2016). The time series of meteorological conditions throughout the sampling period are shown in Figure S5 in Supporting Information S1. During the sampling period, $\text{PM}_{2.5}$ varied from 12.5 to 188.0 $\mu\text{g m}^{-3}$ with an average value of $46.8 \pm 29.0 \mu\text{g m}^{-3}$ and showed higher concentrations in winter ($129.4 \pm 48.1 \mu\text{g m}^{-3}$) and lower concentrations in summer ($32.9 \pm 18.7 \mu\text{g m}^{-3}$). A large amount of precipitation was observed in all seasons except for autumn. Air temperature was lowest in winter ($7.3^\circ\text{C} \pm 4.3^\circ\text{C}$) and highest in summer ($29.3^\circ\text{C} \pm 2.7^\circ\text{C}$). Compared with northern cities in China (Qu et al., 2019), it showed relatively high RH (31%–96%, $75\% \pm 14\%$) in Hangzhou. Boundary layer height (BLH, calculated method is shown in Text S5 in Supporting Information S1) was lower in winter ($865 \pm 280 \text{ m}$) and higher in summer ($1,105 \pm 295 \text{ m}$). Wind speed exhibited the highest value in spring and the average value throughout the year was $2.1 \pm 0.8 \text{ m s}^{-1}$. The wind from the northeast was dominant (45%) from January to October in 2016.

The observations of nitrate concentrations, isotopes of nitrate, and trace gases are shown in Figure 1. During the sampling period, the mass concentration of nitrate varied from 0.02 to 54.3 $\mu\text{g m}^{-3}$ (Figure 1a) and showed similar variation with $\text{PM}_{2.5}$ ($r = 0.81$, $P < 0.01$). NO_3^- was highest in winter ($21.0 \pm 14.3 \mu\text{g m}^{-3}$) and lowest in summer ($3.4 \pm 6.6 \mu\text{g m}^{-3}$). NO_2 was positively correlated with NO_3^- ($r = 0.69$, $P < 0.01$; Table S2 in Supporting Information S1), it showed the maximum value in winter and decreased to less than 10 ppb since 2016 April. Hourly O_3 concentrations varied from 1.5 to 52 ppb and was highest in summer and lowest in winter. The ratio of O_x ($\text{O}_3 + \text{NO}_2$) to CO was normally used to evaluate the oxidation capacity of the atmosphere (Cheng et al., 2008). The O_x/CO ratio varied from 21 to 157 and showed similar seasonal variation with O_3 in this study. Nitrogen oxidation ratio (NOR) ranged from 0 to 0.57, which showed the highest value in winter and decreased to less than 0.1 during July–August in 2016.

The nitrogen isotope of nitrate ($\delta^{15}\text{N}-\text{NO}_3^-$) ranged from -2.9‰ to 18.1‰ with higher values in winter ($9.8\text{‰} \pm 3.2\text{‰}$) and lower values in summer ($5.9\text{‰} \pm 6.0\text{‰}$). The change of $\delta^{15}\text{N}-\text{NO}_3^-$ depends on the seasonal variations of NO_x sources and the nitrogen isotopic fractionation in nitrate production. Interestingly, in marine aerosols, the $\delta^{15}\text{N}-\text{NO}_3^-$ reported by Savarino et al. (2013) (-8.8‰ to -2.9‰) was much lower than the values observed in this work, indicating a different story of nitrate sources in the marine boundary layer (MBL) compared with urban sites. The $\delta^{15}\text{N}$ of NO_x in the emission of coal combustion was relatively higher ($17.9\text{‰} \pm 3.1\text{‰}$; Felix et al., 2012; Heaton, 1990; Zong et al., 2022). The NO_x emitted from nitrification and denitrification normally has lower $\delta^{15}\text{N}$ values ($-43.7\text{‰} \pm 15.9\text{‰}$; Felix & Elliott, 2014; D. Li & Wang, 2008; D. J. Miller et al., 2018; Su et al., 2020; Z. Yu & Elliott, 2017). The nitrogen isotopic fractionation during the $\text{NO}_{x(\text{g})}$ - NO_3^- (p) conversion was associated with air temperature and the nitrate formation pathways, thus it varied a lot in different seasons (Walters & Michalski, 2016). Therefore, the higher values of $\delta^{15}\text{N}-\text{NO}_3^-$ in winter were mainly derived by NO_x sources with enriched isotope compositions and/or larger isotopic fractionation.

The oxygen isotopes of nitrate also showed significant seasonal variations. $\delta^{18}\text{O}-\text{NO}_3^-$ changed from 47.8‰ to 95.0‰ during the sampling period, which was higher in winter ($84.8\text{‰} \pm 6.1\text{‰}$) and lower in summer ($54.0\text{‰} \pm 6.4\text{‰}$) and showed similar tendency with the observations in urban areas reported by Zong et al. (2020). However, the $\delta^{18}\text{O}-\text{NO}_3^-$ values in Hangzhou were much higher than those observed in the MBL

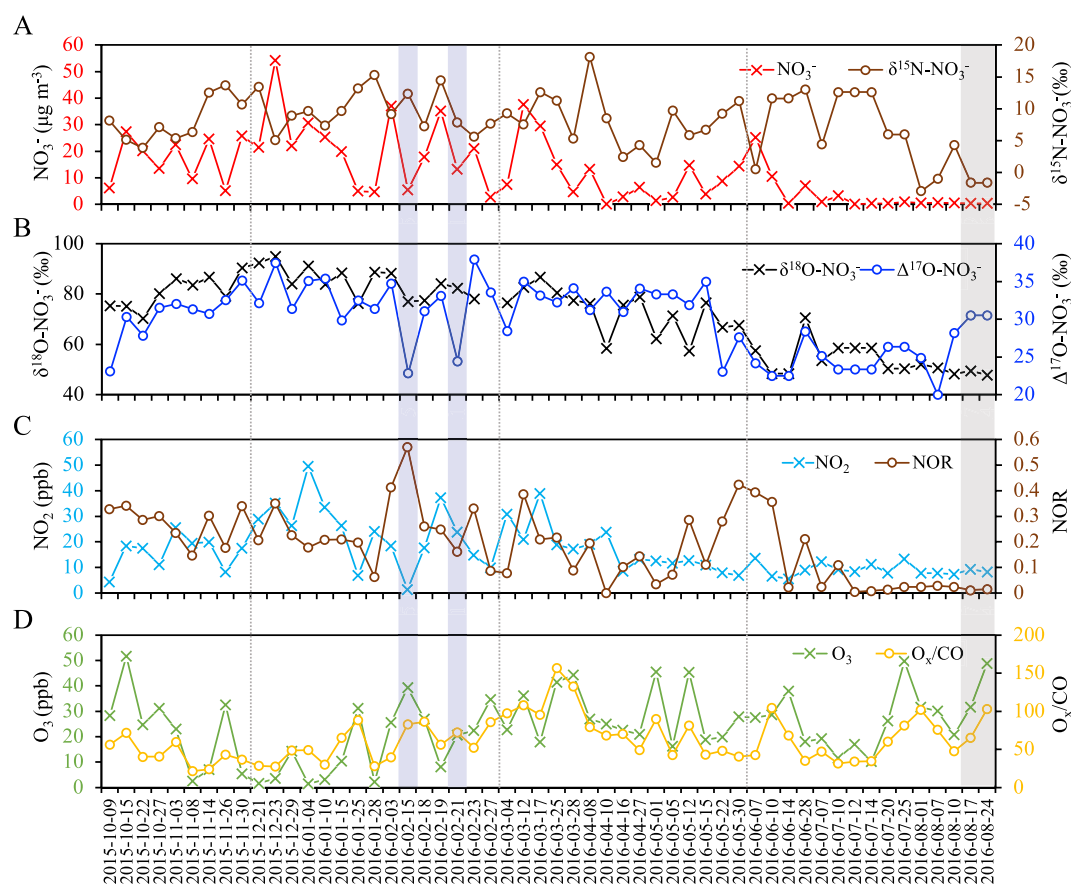


Figure 1. Time series of (a) nitrate (NO_3^-) concentrations and nitrogen isotope of nitrate ($\delta^{15}\text{N}-\text{NO}_3^-$), (b) oxygen isotopes of nitrate ($\delta^{18}\text{O}-\text{NO}_3^-$ and $\Delta^{17}\text{O}-\text{NO}_3^-$), (c) nitrogen dioxide (NO_2) concentrations and NOR values, and (d) ozone (O_3) concentrations and ratios of O_3 to CO (O_3/CO). Blue shades represent the low $\Delta^{17}\text{O}-\text{NO}_3^-$ cases in winter and gray shade represents the high $\Delta^{17}\text{O}-\text{NO}_3^-$ case in summer.

(37.6‰–76.7‰, mean = 61.7‰; Y. Li et al., 2022), indicating different formation mechanisms of nitrate aerosols between urban and marine regions. In this study, $\delta^{18}\text{O}-\text{NO}_3^-$ was positive correlated with $\Delta^{17}\text{O}-\text{NO}_3^-$ ($r = 0.59$, $P < 0.01$). The oxygen isotope anomaly of nitrate ($\Delta^{17}\text{O}-\text{NO}_3^-$) ranged from 20.0‰ to 37.9‰, with an average of $29.5\text{‰} \pm 4.4\text{‰}$. $\Delta^{17}\text{O}-\text{NO}_3^-$ showed similarly high values in winter ($32.2\text{‰} \pm 4.0\text{‰}$), spring ($31.8\text{‰} \pm 3.1\text{‰}$), and autumn ($30.5\text{‰} \pm 3.2\text{‰}$), while relatively lower values in summer ($25.3\text{‰} \pm 3.3\text{‰}$). $\Delta^{17}\text{O}-\text{NO}_3^-$ was within the range of the observation in midlatitudes (Savarino et al., 2007), and similar with previous studies in Beijing ($29.0\text{‰} \pm 4.0\text{‰}$ during winter and $27.3\text{‰} \pm 2.4\text{‰}$ during summer; Fan et al., 2021) and Shanghai (20.5‰ – 31.9‰ ; He et al., 2020). The discrepancy of meteorological conditions in different seasons could partially explain the variation of $\Delta^{17}\text{O}-\text{NO}_3^-$. For example, longer night hours in winter were in favor of nighttime reactions (e.g., NO_3 reactions) to produce nitrate with higher $\Delta^{17}\text{O}-\text{NO}_3^-$. $\Delta^{17}\text{O}-\text{NO}_3^-$ values were lower in summer might be due to the lower particle mass concentrations and therefore the surface area of particles, limiting the heterogeneous uptake of N_2O_5 to produce nitrate (Cai et al., 2017; Zheng et al., 2015). The strong sunlight during the day in summer would accelerate photochemical oxidation reactions, producing nitrate particles with lower $\Delta^{17}\text{O}$ values through the reaction of NO_2 with OH radicals.

3.2. Formation Pathways of Atmospheric Nitrate

Based on the observed $\Delta^{17}\text{O}-\text{NO}_3^-$ values, the contribution of different pathways to nitrate formation were quantified by combining a Bayesian model (Text S3 in Supporting Information S1). The results are shown in Figure 2. During the whole sampling period, the $\text{NO}_2 + \text{OH}$, $\text{N}_2\text{O}_5 + \text{H}_2\text{O}$, and $\text{NO}_3 + \text{HC}/\text{H}_2\text{O}$ pathways contributed, on average, $25\text{‰} \pm 11\text{‰}$, $35\text{‰} \pm 19\text{‰}$, and $40\text{‰} \pm 10\text{‰}$ to nitrate production, respectively (Figure 2a). The

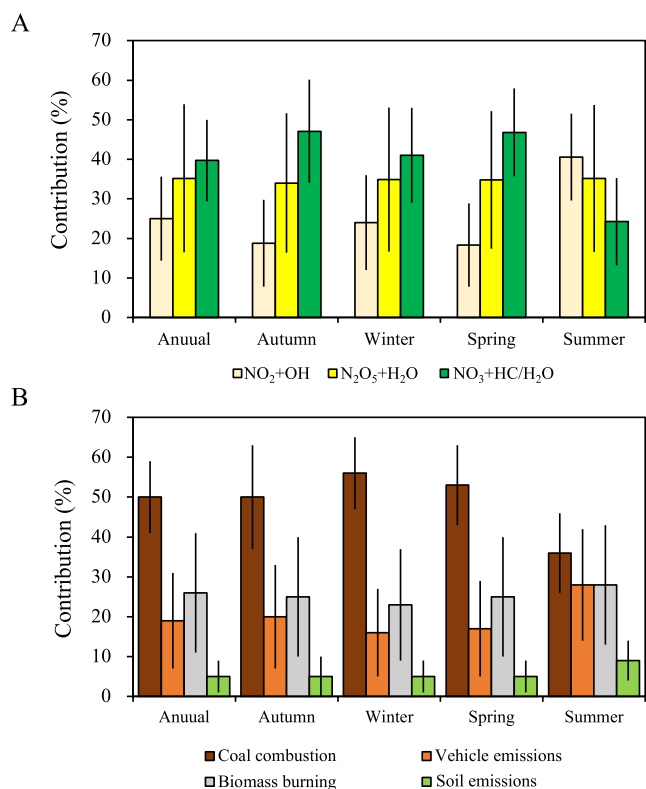


Figure 2. (a) Relative contributions of NO₂ + OH, N₂O₅ + H₂O, and NO₃ + HC/H₂O pathways to nitrate production and (b) relative contributions of NO_x sources to nitrate aerosols after considering the effect of nitrogen isotopic fractionation during the sampling period.

nocturnal chemistry (including NO₃ + HC/H₂O and N₂O₅ + H₂O pathways) was predominant (annual mean value: 75%) in nitrate production throughout the year and showed higher contributions in the autumn (81%), winter (76%), and spring (82%) than that in summer (59%). This result was similar to the previous studies in Beijing (Fan et al., 2021; Y. L. Wang et al., 2019). The contribution of daytime chemistry (NO₂ + OH pathway) changed oppositely with nocturnal pathways, which averaged at 41% in summer and 18%–24% in other three seasons. In addition, the formation mechanisms of nitrate aerosols were found to be different at different pollution levels (Figure 3a). Daytime chemistry dominated the nitrate production in clean air (NO₃⁻ < 1 μg m⁻³). With the increase of pollution level, nocturnal chemistry became the major contributor of nitrate aerosols. Particularly, the NO₃ + HC/H₂O pathway contributed ~59% to nitrate production in the most polluted days (NO₃⁻ > 35 μg m⁻³).

3.3. Nitrogen Isotopic Fractionation Effects

The Δ¹⁵N between NO_{x(g)} and NO_{3⁻(p)} ranged from -7.1‰ to 10.5‰ with an average of 2.9‰ ± 5.5‰ (Figure S6 in Supporting Information S1). The Δ¹⁵N in autumn, winter, spring, and summer was 0.5‰ ± 5.9‰, 2.7‰ ± 5.0‰, 1.8‰ ± 4.7‰, and 5.5‰ ± 5.2‰, respectively. Our estimated Δ¹⁵N was similar with the previous result at a megacity in northern China (Z. Li et al., 2019). The discrepancy of Δ¹⁵N in different seasons was caused by the seasonal variation of isotopic fractionation in each process from NO_{x(g)} to NO_{3⁻(p)}. In NO_x cycle, the nitrogen isotopic fractionation between NO_x and NO₂ (ε_{NO₂}) varied from 0.4‰ to 6.7‰ with an average value of 3.1‰ ± 1.4‰, which was within the estimation (-5‰ to 20‰) of a previous study (J. Li et al., 2020). ε_{NO₂} was lower in winter (1.9‰ ± 1.2‰) and higher in summer (4.1‰ ± 1.3‰). ε_{NO₂} was affected by the variation of *A* and *f*(NO₂) (Equation 6). A smaller *A* represents a more significant impact of the PHIFE and the KIE than the EIE on ε_{NO₂} (Michalski et al., 2004; C. E.

Miller & Yung, 2000), which would be exhibited with high NO and low *j*(NO₂) (controlled by the solar elevation angle; Equations S5 and S6 in Supporting Information S1) and resulted in higher values of ε_{NO₂}. And smaller *f*(NO₂) would result in higher values of ε_{NO₂}. Since higher *j*(NO₂) and lower NO were observed in summer, the lower *f*(NO₂) was the main reason of the higher ε_{NO₂} in summer. When the mixing ratio of NO_x increased to larger than 20 ppb, EIE was dominant in the nitrogen isotopic fractionation between NO_x and NO₂ (J. Li et al., 2020).

The average value of the EIE between NO_{2(g)} and HNO_{3(g)} (Δ¹⁵N₂) was calculated to be 2.0‰ ± 5.0‰ with the range of -7.3‰ to 9.6‰. Δ¹⁵N₂ was relatively higher in summer (3.8‰ ± 4.5‰) compared with the other seasons. Δ¹⁵N₂ was affected by the isotopic fractionation factors (i.e., ε_{NO₃} and ε_{N₂O₅}) and the contributions of nitrate formation pathways, both varied in different seasons. ε_{NO₃} was higher in summer (-18.0‰) and lower in winter (-18.9‰). ε_{N₂O₅} changed oppositely with higher values in winter (28.6‰) and lower values in summer (25.2‰). Both isotopic fractionation factors were affected by the variation of air temperatures (Equation 9). Furthermore, the lower contribution of NO₃ + HC pathways in summer (26%) than other seasons (41%–49%) finally resulted in the higher Δ¹⁵N₂ values. The seasonal variation of δ¹⁵N-NO_x was mainly affected by the composition of NO_x sources in different seasons. The obtained δ¹⁵N-NO_x was then applied in the NO_x source apportionment in following sections.

3.4. Source Contributions to Atmospheric Nitrate

Coal combustion, vehicle emissions, BB, and soil emissions (NO_x emitted from nitrification/denitrification in farmland and soil) were taken as the possible sources in Hangzhou, due to the correlation of nitrate with various tracers of NO_x sources (Text S6 and Table S2 in Supporting Information S1). The nitrate source apportionment was accomplished with a Bayesian model and typical nitrogen isotope values of NO_x sources reported in previous studies (Text S3 and Table S3 in Supporting Information S1). Over the whole year, coal combustion was the

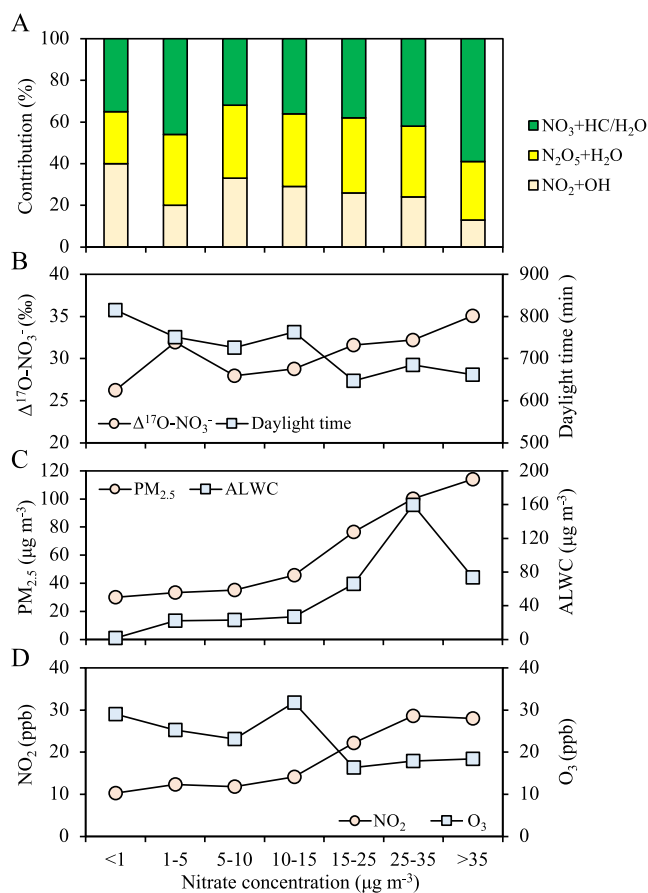


Figure 3. Changes of (a) relative contribution of each formation pathway, (b) $\Delta^{17}\text{O}-\text{NO}_3^-$ and daylight time, (c) $\text{PM}_{2.5}$ and ALWC, and (d) NO_2 and O_3 under different nitrate levels.

largest contributor ($50\% \pm 9\%$) of nitrate aerosols (Figure 2b), which agreed with the positive correlation between NO_3^- and SO_2 ($r = 0.55$, $P < 0.001$; Lang et al., 2012). In addition, mobile emissions, BB, and soil emissions contributed $19\% \pm 12\%$, $26\% \pm 15\%$, and $5\% \pm 4\%$, respectively, to nitrate aerosols (Figure 2b). Obvious seasonal variation of nitrate sources was found. The contribution of coal combustion was higher in winter ($56\% \pm 9\%$), spring ($53\% \pm 10\%$), and autumn ($50\% \pm 13\%$) than in summer ($36\% \pm 10\%$). In contrary, the contribution of soil emission was higher in summer ($9\% \pm 5\%$) than in winter, spring, and autumn ($\sim 5\%$).

4. Discussion

4.1. Influence Factors of Nitrate Production

Various reasons could influence the production of particulate nitrate. First, the atmospheric oxidation capacity would be different in various seasons or at different pollution levels. Nitrate production depends on the concentrations of oxidants in the atmosphere (e.g., O_3 and OH radicals) which formation requires the existence of the sunlight. The mixing ratios of OH radicals and O_3 represent the oxidation capacity of the atmosphere, which are normally higher in summer with longer daylight hours (Kumar & Sinha, 2021; Platt et al., 1980). In winter, the mixing ratio of O_3 was much higher than OH and HO_2/RO_2 radicals (Fleming et al., 2006) and the reaction time (dark time) of NO_3 and N_2O_5 reactions is much longer than summer (Figure S5 in Supporting Information S1), which made the nocturnal chemistry dominant in the nitrate production. In addition, the decline of daylight time was found along with the increase of nitrate pollution (Figure 3b), which provided favorable environment for the occurrence of nocturnal chemistry in haze days.

Second, heterogeneous chemistry would increase in polluted days. According to a previous study, particles collected in Beijing haze episodes turn into liquid state from semisolid, when RH increased to be more than 60%, such that the liquid particles might readily take up inorganic pollutants (Y. Liu et al., 2017). The aerosol surface could increase with the mass concentration of $\text{PM}_{2.5}$, which would provide the interface and accelerate the heterogeneous

reactions (Cai et al., 2017; Y. L. Wang et al., 2019). In this work, the increasing contributions of $\text{NO}_3 + \text{HC}/\text{H}_2\text{O}$ and $\text{N}_2\text{O}_5 + \text{H}_2\text{O}$ pathways were observed with aerosols liquid water content (ALWC, calculation method is shown in Text S7 in Supporting Information S1) and $\text{PM}_{2.5}$ (Figure 3c). This suggested that the enhanced hydrolysis reactions of NO_3 and N_2O_5 on particle surface produced a large amount of nitrate aerosols in the humid and polluted atmosphere. In this work, O_3 concentration decreased and NO_2 concentration increased when nitrate $\geq 15 \mu\text{g m}^{-3}$ (Figure 3d), which might be ascribed to the insufficient daylight restrained the photolysis of NO_2 and NO_3 radicals and promoted the formation of NO_3 and N_2O_5 radicals in the polluted atmosphere.

Besides that, a few cases in winter (e.g., 15 and 21 February) with extremely low $\Delta^{17}\text{O}-\text{NO}_3^-$ ($22\% \sim 25\%$, Figure 1b) represent a large contribution of $\text{NO}_2 + \text{OH}$ reaction to nitrate formation. The case on 15 February was under the circumstances when the north wind was dominant, and the daily average wind speed increased to 6 m s^{-1} (Figure S5 in Supporting Information S1). The results show that the mass concentration of $\text{PM}_{2.5}$ was $13.7 \mu\text{g m}^{-3}$, indicating the accumulated pollution was scavenged by the north wind. The low particles were not able to provide sufficient reaction sites for various heterogeneous reactions, especially with relatively low RH (36%; Figure S5 in Supporting Information S1). In addition, NO_2 was extremely low ($< 1.5 \text{ ppb}$) with relatively high value of NOR (0.59; Figure 1c), which suggested fast nitrate formation through $\text{NO}_2 + \text{OH}$ reaction in the clean atmosphere during the day. As for the case on 21 February, the sample collection was conducted during the rainfall. As a result, the $\text{PM}_{2.5}$ and NO_3^- decreased to 65 and $13.1 \mu\text{g m}^{-3}$. Meanwhile, O_3 increased to 20.7 ppb and the ALWC was extremely low ($4.9 \mu\text{g m}^{-3}$; Figure 1d and Figure S5 in Supporting Information S1). This phenomenon revealed the enhanced photochemical capabilities of atmosphere and the less importance of heterogeneous reactions in the fresh nitrate production when the air pollutants were cleaned by the rain, which was supported by the previous study of oxygen isotopes of nitrate in precipitation (Y.-L. Zhang et al., 2022).

In summer, the high values of $\Delta^{17}\text{O}-\text{NO}_3^-$ ($>30\text{‰}$) were found on 17 and 24 August (Figure 1b), indicating the high contribution of $\text{NO}_2 + \text{HC}/\text{H}_2\text{O}$ pathway. This result was very different from others during the whole summer period, in which nitrate was mainly produced by the $\text{NO}_2 + \text{OH}$ pathway. On these 2 days, the wind both came from southeast direction, the average wind speed was around 4 m s^{-1} , and the BLH was relatively low ($\sim 720 \text{ m}$; Figure S5 in Supporting Information S1). These conditions were conducive to the stable state of the atmosphere. At the same time, high O_3 concentrations were observed (Figure 1d), potentially resulting in the production of NO_3 radicals and then the reaction of NO_3 with hydrocarbons (Asaf et al., 2010; Vrekoussis et al., 2007).

4.2. Emission Sources of Atmospheric Nitrate in Hangzhou

The dominance of coal combustion to atmospheric nitrate agrees with the observation result in Shanghai reported by Zong et al. (2020) and the emission inventories that indicting coal to be the dominant source of NO_x in China (F. Liu et al., 2016) as well as the YRD (C. Huang et al., 2011). Based on Multiresolution Emission Inventory for China (MEIC, <http://www.meicmodel.org/>), the coal-related emission sources, industry, and power plant were the major NO_x emission sectors in the YRD (N. Wang et al., 2019). In addition, the footprint of aerosols during the sampling period suggested that air pollutants at the receptor site were not only from local emissions but also affected by regional transported pollution from neighboring provinces like Jiangsu, Anhui, as well as Jiangxi (Lin et al., 2022). The coal materials produced in these provinces could also contribute nitrate aerosols to the receptor site. Our result indicated that coal combustion was still a dominant source of atmospheric NO_3^- . Strict control measures of reduction in NO_x emissions from coal-fired power plants and industrial emissions in local Hangzhou and its neighboring provinces were still needed.

Our results also showed vehicle exhausts was a nonneglected NO_x in urban cities (C. Huang et al., 2011), and BB was also an important source of nitrate aerosols in the YRD (Yang & Zhao, 2019). Previously, fossil fuel combustion was estimated to account for 96% of total NO_x emission in China (Gu et al., 2012). The ratio of fossil-fuel-produced nitrate to non-fossil-fuel-derived nitrate in Hangzhou was approximately 2.2, which was much higher than those in megacities in southern China like Chengdu (~ 1.4) and Guangzhou (~ 1.6), but lower than the value in Changchun city (~ 3.3) in northeast China (Zhao et al., 2021; Zong et al., 2020). This suggested that the fossil fuel consumption in southern and eastern China was lower than the northeast China.

The obvious seasonal variation of nitrate sources in this work was consistent with the results in an aerosol study in Shanghai (Zong et al., 2020) and a precipitation study in Ningbo (Shi et al., 2021). The higher contribution of coal combustion during cold seasons might be related to the coal-fired heating in rural areas in Hangzhou and surrounding regions. The increasing soil NO_x emission in summer was due to the active microbial processes in soils under high air temperature condition, combining with the effects from a large garden (Hangzhou Botanical Garden, area = 2.85 km^2) locating less than 1 km away from the sampling site. In addition, the contribution of BB was almost constant (23%–28%) throughout the year, which was coincided with the intense open fire spots observed in Hangzhou in four seasons (Figure S7 in Supporting Information S1). To analyze the influence of fractionation effects on nitrate source apportionments, the nitrate sources were estimated without consideration of fractionation effects between $\text{NO}_{x(\text{g})}$ and $\text{NO}_{3^-(\text{p})}$. As shown in Figure S8 in Supporting Information S1, the contributions of nitrate sources without considering the $\Delta^{15}\text{N}$ produced the same contribution pattern with the results with considering the fractionation effects for the entire year. However, when without considering the $\Delta^{15}\text{N}$, the contribution of coal combustion was higher than that with considering the fractionation effects. The contributions of mobile and soil emissions in summer were lower than those with considering the $\Delta^{15}\text{N}$. The results indicated that the ignorance of isotopic fractionation normally caused the overestimation or underestimation of the contribution of NO_x source.

5. Conclusions

Multiple isotope compositions of nitrate ($\delta^{15}\text{N}-\text{NO}_3^-$, $\delta^{18}\text{O}-\text{NO}_3^-$, and $\Delta^{17}\text{O}-\text{NO}_3^-$) in $\text{PM}_{2.5}$ collected in Hangzhou from 2015 to 2016 were determined in this study. The contribution of each nitrate formation pathway was estimated using the $\Delta^{17}\text{O}-\text{NO}_3^-$ observation. The nitrogen isotopic fractionation ($\Delta^{15}\text{N}$) during the nitrate production and the $\delta^{15}\text{N}-\text{NO}_x$ were calculated based on the results of nitrate formation mechanisms. And the NO_x source apportionment was conducted in various seasons with a Bayesian model. The results showed that $\text{NO}_2 + \text{OH}$, $\text{N}_2\text{O}_5 + \text{H}_2\text{O}$, and $\text{NO}_3 + \text{HC}/\text{H}_2\text{O}$ pathways contributed $25\% \pm 11\%$, $35\% \pm 19\%$, and $40\% \pm 10\%$ to nitrate

production, respectively. Nocturnal chemistry (including $\text{NO}_3 + \text{HC}/\text{H}_2\text{O}$ and $\text{N}_2\text{O}_5 + \text{H}_2\text{O}$ pathways) showed higher contributions in cold seasons and contributed equally with $\text{NO}_2 + \text{OH}$ pathway to nitrate formation in summer. In addition, the contributions of $\text{NO}_3 + \text{HC}/\text{H}_2\text{O}$ and $\text{N}_2\text{O}_5 + \text{H}_2\text{O}$ pathways increased obviously with ALWC and $\text{PM}_{2.5}$, suggesting the enhanced hydrolysis reactions of NO_3 and N_2O_5 on particle surface produced a large amount of nitrate aerosols in Hangzhou. Coal combustion ($50\% \pm 9\%$) was the most important nitrate source in Hangzhou. Coal combustion and soil emission showed significant seasonal variation due to the coal consumption in cold seasons and active soil microbial processes in summer.

The uncertainties of NO_x source apportionment in this study were mainly attributed to the neglect of difference between $\delta^{15}\text{N}\text{-HNO}_3$ and $\delta^{15}\text{N}\text{-NO}_3^-$ and the lack of precise typical nitrogen isotopic values of NO_x sources. Although the uncertainties are nonnegligible, it provides an easy and fast approach to characterize the NO_x sources combined with observations in ambient environment. Consequently, the detection of dominant NO_x sources in the YRD and the studies on the nitrogen isotopic fractionation between $\text{HNO}_{3(\text{g})}$ and $\text{NO}_3^-_{(\text{p})}$ are required in the future for a better understanding of the composition of NO_x sources in China.

Conflict of Interest

The authors declare no conflicts of interest relevant to this study.

Data Availability Statement

Data: the observation data of chemical species, meteorological parameters, and isotopes in this work are available at <https://doi.org/10.17605/OSF.IO/ASY28> (Fan et al., 2023). *Software:* the fraction of NO_2 oxidized from O_3 (α) was simulated by the i_{N} RACM model developed by Fang et al. (2021), which is available for public use at <https://mygeohub.org/tools/sbox/>. *Software:* the NO_2 photolysis rate ($j(\text{NO}_2)$) was calculated with the online model of the tropospheric ultraviolet and visible (TUV) radiation model (TUV5.3.2) and is available at <https://www2.acom.ucar.edu/modeling/tuv-download> (Madronich & Flocke, 1999). *Software:* the source apportionment of nitrate aerosols was resolved by the SIAR model (version 4.2), which can be downloaded from <https://cran.r-project.org/src/contrib/Archive/siar/> (Parnell & Jackson, 2011). *Software:* the back trajectories data were calculated with hybrid single-particle Lagrangian integrated trajectory model, developing by the United States National Oceanic and Atmospheric Administration (NOAA; https://www.ready.noaa.gov/HYSPLIT_hytrial.php; NOAA, 2022). *Software:* the aerosol liquid water content (ALWC) was calculated using the ISORROPIA-II model, which can be obtained at http://wiki.seas.harvard.edu/geos-chem/index.php?title=ISORROPIA_II (Fountoukis & Nenes, 2007).

References

- Alexander, B., Hastings, M. G., Allman, D. J., Dachs, J., Thornton, J. A., & Kunasek, S. A. (2009). Quantifying atmospheric nitrate formation pathways based on a global model of the oxygen isotopic composition ($\Delta^{17}\text{O}$) of atmospheric nitrate. *Atmospheric Chemistry and Physics*, 9(14), 5043–5056. <https://doi.org/10.5194/acp-9-5043-2009>
- Alexander, B., Sherwen, T., Holmes, C. D., Fisher, J. A., Chen, Q., Evans, M. J., & Kasibhatla, P. (2020). Global inorganic nitrate production mechanisms: Comparison of a global model with nitrate isotope observations. *Atmospheric Chemistry and Physics*, 20(6), 3859–3877. <https://doi.org/10.5194/acp-20-3859-2020>
- Asaf, D., Tas, E., Pedersen, D., Peleg, M., & Luria, M. (2010). Long-term measurements of NO_3 radical at a semiarid urban site: 2. Seasonal trends and loss mechanisms. *Environmental Science & Technology*, 44(15), 5901–5907. <https://doi.org/10.1021/es100967z>
- Cai, R., Yang, D., Fu, Y., Wang, X., Li, X., Ma, Y., et al. (2017). Aerosol surface area concentration: A governing factor in new particle formation in Beijing. *Atmospheric Chemistry and Physics*, 17(20), 12327–12340. <https://doi.org/10.5194/acp-17-12327-2017>
- Chen, Z., Chen, D., Zhao, C., Kwan, M.-P., Cai, J., Zhuang, Y., et al. (2020). Influence of meteorological conditions on $\text{PM}_{2.5}$ concentrations across China: A review of methodology and mechanism. *Environment International*, 139, 105558. <https://doi.org/10.1016/j.envint.2020.105558>
- Cheng, Y., Wang, X., Liu, Z., Bai, Y., & Li, J. (2008). A new method for quantitatively characterizing atmospheric oxidation capacity. *Science in China, Series B: Chemistry*, 51(11), 1102–1109. <https://doi.org/10.1007/s11426-008-0119-z>
- Ding, A. J., Fu, C. B., Yang, X. Q., Sun, J. N., Zheng, L. F., Xie, N. Y., et al. (2013). Ozone and fine particle in the western Yangtze River Delta: An overview of 1 yr data at the SORPES station. *Atmospheric Chemistry and Physics*, 13(11), 5813–5830. <https://doi.org/10.5194/acp-13-5813-2013>
- Elliott, E. M., Kendall, C., Boyer, E. W., Burns, D. A., Lear, G. G., Golden, H. E., et al. (2009). Dual nitrate isotopes in dry deposition: Utility for partitioning NO_x source contributions to landscape nitrogen deposition. *Journal of Geophysical Research*, 114, G04020. <https://doi.org/10.1029/2008JG000889>
- Elliott, E. M., Kendall, C., Wankel, S. D., Burns, D. A., Boyer, E. W., Harlin, K., et al. (2007). Nitrogen isotopes as indicators of NO_x source contributions to atmospheric nitrate deposition across the midwestern and northeastern United States. *Environmental Science & Technology*, 41(22), 7661–7667. <https://doi.org/10.1021/es070898t>

Acknowledgments

This study is supported by the National Natural Science Foundation of China (42207136, 42192512, and 42273087), the Research Grants Council of the Hong Kong Special Administrative Region via the NSFC/RGC Joint Research Scheme (N_PolyU530/20), and the Hong Kong Scholars Program (XJ2021026).

- Elliott, E. M., Yu, Z., Cole, A. S., & Coughlin, J. G. (2019). Isotopic advances in understanding reactive nitrogen deposition and atmospheric processing. *Science of the Total Environment*, 662, 393–403. <https://doi.org/10.1016/j.scitotenv.2018.12.177>
- Fan, M.-Y., Zhang, W., Zhang, Y.-L., Li, J., Fang, H., Cao, F., et al. (2023). Formation mechanisms and source apportionments of nitrate aerosols in a megacity of eastern China based on multiple isotope observations [Dataset]. OSF. <https://doi.org/10.17605/OSF.IO/ASY28>
- Fan, M.-Y., Zhang, Y.-L., Lin, Y.-C., Chang, Y.-H., Cao, F., Zhang, W.-Q., et al. (2019). Isotope-based source apportionment of nitrogen-containing aerosols: A case study in an industrial city in China. *Atmospheric Environment*, 212, 96–105. <https://doi.org/10.1016/j.atmosenv.2019.05.020>
- Fan, M.-Y., Zhang, Y.-L., Lin, Y.-C., Hong, Y., Zhao, Z.-Y., Sun, Y., et al. (2020). Changes of emission sources to nitrate aerosols in Beijing after the clean air actions: Evidence from dual isotope compositions. *Journal of Geophysical Research: Atmospheres*, 125, e2019JD031998. <https://doi.org/10.1029/2019JD031998>
- Fan, M.-Y., Zhang, Y.-L., Lin, Y.-C., Hong, Y., Zhao, Z.-Y., Xie, F., et al. (2021). Important role of NO₃ radical to nitrate formation aloft in urban Beijing: Insights from triple oxygen isotopes measured at the tower. *Environmental Science & Technology*, 56(11), 6870–6879. <https://doi.org/10.1021/acs.est.1c02843>
- Fang, H., Walters, W. W., Mase, D., & Michalski, G. (2021). i₃RACM: Incorporating ¹⁵N into the Regional Atmospheric Chemistry Mechanism (RACM) for assessing the role photochemistry plays in controlling the isotopic composition of NO_x, NO_y, and atmospheric nitrate. *Geoscientific Model Development*, 14(8), 5001–5022. <https://doi.org/10.5194/gmd-14-5001-2021>
- Felix, J. D., & Elliott, E. M. (2014). Isotopic composition of passively collected nitrogen dioxide emissions: Vehicle, soil and livestock source signatures. *Atmospheric Environment*, 92, 359–366. <https://doi.org/10.1016/j.atmosenv.2014.04.005>
- Felix, J. D., Elliott, E. M., & Shaw, S. L. (2012). Nitrogen isotopic composition of coal-fired power plant NO_x: Influence of emission controls and implications for global emission inventories. *Environmental Science & Technology*, 46(6), 3528–3535. <https://doi.org/10.1021/es203355v>
- Feng, J., Chan, C. K., Fang, M., Hu, M., He, L., & Tang, X. (2006). Characteristics of organic matter in PM_{2.5} in Shanghai. *Chemosphere*, 64(8), 1393–1400. <https://doi.org/10.1016/j.chemosphere.2005.12.026>
- Fibiger, D. L., & Hastings, M. G. (2016). First measurements of the nitrogen isotopic composition of NO_x from biomass burning. *Environmental Science & Technology*, 50(21), 11569–11574. <https://doi.org/10.1021/acs.est.6b03510>
- Fleming, Z. L., Monks, P. S., Rickard, A. R., Bandy, B. J., Brough, N., Green, T. J., et al. (2006). Seasonal dependence of peroxy radical concentrations at a Northern Hemisphere marine boundary layer site during summer and winter: Evidence for radical activity in winter. *Atmospheric Chemistry and Physics*, 6(12), 5415–5433. <https://doi.org/10.5194/acp-6-5415-2006>
- Fountoukis, C., & Nenes, A. (2007). ISORROPIA II: A computationally efficient thermodynamic equilibrium model for K⁺-Ca²⁺-Mg²⁺-NH₄⁺-Na⁺-SO₄²⁻-NO₃⁻-Cl⁻-H₂O aerosols. *Atmospheric Chemistry and Physics*, 7(17), 4639–4659. <https://doi.org/10.5194/acp-7-4639-2007>
- Gao, C., Shi, J.-W., Fan, Z., Gao, G., & Niu, C. (2018). Sulfur and water resistance of Mn-based catalysts for low-temperature selective catalytic reduction of NO_x: A review. *Catalysts*, 8(1), 11. <https://doi.org/10.3390/catal8010011>
- Gu, B., Ge, Y., Ren, Y., Luo, W., Jiang, H., Gu, B., et al. (2012). Atmospheric reactive nitrogen in China: Sources, recent trends, and damage costs. *Environmental Science & Technology*, 46(17), 9420–9427. <https://doi.org/10.1021/es301446g>
- He, P., Xie, Z., Yu, X., Wang, L., Kang, H., & Yue, F. (2020). The observation of isotopic compositions of atmospheric nitrate in Shanghai China and its implication for reactive nitrogen chemistry. *Science of the Total Environment*, 714, 136727. <https://doi.org/10.1016/j.scitotenv.2020.136727>
- Heaton, T. H. E. (1990). ¹⁵N/¹⁴N ratios of NO_x from vehicle engines and coal-fired power stations. *Tellus B: Chemical and Physical Meteorology*, 42(3), 304–307. <https://doi.org/10.1034/j.1600-0889.1990.00007.x-i1>
- Huang, C., Chen, C. H., Li, L., Cheng, Z., Wang, H. L., Huang, H. Y., et al. (2011). Emission inventory of anthropogenic air pollutants and VOC species in the Yangtze River Delta region, China. *Atmospheric Chemistry and Physics*, 11(9), 4105–4120. <https://doi.org/10.5194/acp-11-4105-2011>
- Huang, R.-J., Zhang, Y., Bozzetti, C., Ho, K.-F., Cao, J.-J., Han, Y., et al. (2014). High secondary aerosol contribution to particulate pollution during haze events in China. *Nature*, 514(7521), 218–222. <https://doi.org/10.1038/nature13774>
- Ishino, S., Hattori, S., Savarino, J., Jourdain, B., Preunkert, S., Legrand, M., et al. (2017). Seasonal variations of triple oxygen isotopic compositions of atmospheric sulfate, nitrate, and ozone at Dumont d'Urville, coastal Antarctica. *Atmospheric Chemistry and Physics*, 17(5), 3713–3727. <https://doi.org/10.5194/acp-17-3713-2017>
- Jaeglé, L., Steinberger, L., Martin, R. V., & Chance, K. (2005). Global partitioning of NO_x sources using satellite observations: Relative roles of fossil fuel combustion, biomass burning and soil emissions. *Faraday Discussions*, 130, 407–423. <https://doi.org/10.1039/B502128F>
- Kumar, V., & Sinha, V. (2021). Season-wise analyses of VOCs, hydroxyl radicals and ozone formation chemistry over north-west India reveal isoprene and acetaldehyde as the most potent ozone precursors throughout the year. *Chemosphere*, 283, 131184. <https://doi.org/10.1016/j.chemosphere.2021.131184>
- Lang, J., Cheng, S., Wei, W., Zhou, Y., Wei, X., & Chen, D. (2012). A study on the trends of vehicular emissions in the Beijing–Tianjin–Hebei (BTH) region, China. *Atmospheric Environment*, 62, 605–614. <https://doi.org/10.1016/j.atmosenv.2012.09.006>
- Li, D., & Wang, X. (2008). Nitrogen isotopic signature of soil-released nitric oxide (NO) after fertilizer application. *Atmospheric Environment*, 42(19), 4747–4754. <https://doi.org/10.1016/j.atmosenv.2008.01.042>
- Li, H., Zhang, Q., Zheng, B., Chen, C., Wu, N., Guo, H., et al. (2018). Nitrate-driven urban haze pollution during summertime over the North China Plain. *Atmospheric Chemistry and Physics*, 18(8), 5293–5306. <https://doi.org/10.5194/acp-18-5293-2018>
- Li, J., Zhang, X., Orlando, J., Tyndall, G., & Michalski, G. (2020). Quantifying the nitrogen isotope effects during photochemical equilibrium between NO and NO₂: Implications for δ¹⁵N in tropospheric reactive nitrogen. *Atmospheric Chemistry and Physics*, 20(16), 9805–9819. <https://doi.org/10.5194/acp-20-9805-2020>
- Li, Y., Shi, G., Chen, Z., Lan, M., Ding, M., Li, Z., & Hastings, M. G. (2022). Significant latitudinal gradient of nitrate production in the marine atmospheric boundary layer of the Northern Hemisphere. *Geophysical Research Letters*, 49, e2022GL100503. <https://doi.org/10.1029/2022GL100503>
- Li, Z., Walters, W. W., Hastings, M. G., Zhang, Y., Song, L., Liu, D., et al. (2019). Nitrate isotopic composition in precipitation at a Chinese megacity: Seasonal variations, atmospheric processes, and implications for sources. *Earth and Space Science*, 6, 2200–2213. <https://doi.org/10.1029/2019EA000759>
- Lin, Y.-C., Yu, M., Xie, F., & Zhang, Y. (2022). Anthropogenic emission sources of sulfate aerosols in Hangzhou, East China: Insights from isotope techniques with consideration of fractionation effects between gas-to-particle transformations. *Environmental Science & Technology*, 56(7), 3905–3914. <https://doi.org/10.1021/acs.est.1c05823>
- Lin, Y.-C., Zhang, Y.-L., Yu, M., Fan, M.-Y., Xie, F., Zhang, W.-Q., et al. (2021). Formation mechanisms and source apportionments of airborne nitrate aerosols at a Himalayan–Tibetan Plateau site: Insights from nitrogen and oxygen isotopic compositions. *Environmental Science & Technology*, 55(18), 12261–12271. <https://doi.org/10.1021/acs.est.1c03957>

- Liu, F., Zhang, Q., van der A, R. J., Zheng, B., Tong, D., Yan, L., et al. (2016). Recent reduction in NO_x emissions over China: Synthesis of satellite observations and emission inventories. *Environmental Research Letters*, 11(11), 114002. <https://doi.org/10.1088/1748-9326/11/11/114002>
- Liu, Y., Wu, Z., Wang, Y., Xiao, Y., Gu, F., Zheng, J., et al. (2017). Submicrometer particles are in the liquid state during heavy haze episodes in the urban atmosphere of Beijing, China. *Environmental Science and Technology Letters*, 4(10), 427–432. <https://doi.org/10.1021/acs.estlett.7b00352>
- Lu, K., Guo, S., Tan, Z., Wang, H., Shang, D., Liu, Y., et al. (2019). Exploring atmospheric free-radical chemistry in China: The self-cleansing capacity and the formation of secondary air pollution. *National Science Review*, 6(3), 579–594. <https://doi.org/10.1093/nsr/nwy073>
- Madronich, S., & Flocke, S. (1999). The role of solar radiation in atmospheric chemistry. In *Environmental photochemistry. The handbook of environmental chemistry (reactions and processes)* (Vol. 2/2L, pp. 1–26). Springer. https://doi.org/10.1007/978-3-540-69044-3_1
- Martin, R. V., Jacob, D. J., Chance, K., Kurosu, T. P., Palmer, P. I., & Evans, M. J. (2003). Global inventory of nitrogen oxide emissions constrained by space-based observations of NO₂ columns. *Journal of Geophysical Research*, 108(D17), 4537. <https://doi.org/10.1029/2003JD003453>
- Michalski, G., Bhattacharya, S. K., & Mase, D. F. (2012). Oxygen isotope dynamics of atmospheric nitrate and its precursor molecules. In M. Baskaran (Ed.), *Handbook of environmental isotope geochemistry* (Vol. I, pp. 613–635). Springer Berlin Heidelberg. https://doi.org/10.1007/978-3-642-10637-8_30
- Michalski, G., Meixner, T., Fenn, M., Hernandez, L., Sirulnik, A., Allen, E., & Thiemens, M. (2004). Tracing atmospheric nitrate deposition in a complex semiarid ecosystem using Δ¹⁷O. *Environmental Science & Technology*, 38(7), 2175–2181. <https://doi.org/10.1021/es034980+>
- Michalski, G., Scott, Z., Kabling, M., & Thiemens, M. H. (2003). First measurements and modeling of Δ¹⁷O in atmospheric nitrate. *Geophysical Research Letters*, 30(16), 1870. <https://doi.org/10.1029/2003GL017015>
- Miller, C. E., & Yung, Y. L. (2000). Photo-induced isotopic fractionation. *Journal of Geophysical Research*, 105(D23), 29039–29051. <https://doi.org/10.1029/2000JD900388>
- Miller, D. J., Chai, J., Guo, F., Dell, C. J., Karsten, H., & Hastings, M. G. (2018). Isotopic composition of in situ soil NO_x emissions in manure-fertilized cropland. *Geophysical Research Letters*, 45, 12058–12066. <https://doi.org/10.1029/2018GL079619>
- Ming, L., Jin, L., Li, J., Fu, P., Yang, W., Liu, D., et al. (2017). PM_{2.5} in the Yangtze River Delta, China: Chemical compositions, seasonal variations, and regional pollution events. *Environmental Pollution*, 223, 200–212. <https://doi.org/10.1016/j.envpol.2017.01.013>
- NOAA. (2022). Hybrid single-particle Lagrangian integrated trajectory model, developed by the United States National Oceanic and Atmospheric Administration [Software]. National Oceanic and Atmospheric Administration. Retrieved from <https://www.Ready.noaa.gov/HYSPLIT.php>
- Parnell, A., & Jackson, A. (2011). SIAR: Stable isotope analysis in R [Software]. MixSIAR - Bayesian Mixing Models for Stable Isotopes. Retrieved from <https://cran.r-project.org/src/contrib/Archive/siar/>
- Platt, U., Perner, D., Harris, G. W., Winer, A. M., & Pitts, J. N. (1980). Observations of nitrous acid in an urban atmosphere by differential optical absorption. *Nature*, 285(5763), 312–314. <https://doi.org/10.1038/285312a0>
- Qu, Y., Chen, Y., Liu, X., Zhang, J., Guo, Y., & An, J. (2019). Seasonal effects of additional HONO sources and the heterogeneous reactions of N₂O₅ on nitrate in the North China Plain. *Science of the Total Environment*, 690, 97–107. <https://doi.org/10.1016/j.scitotenv.2019.06.436>
- Rohrer, F., & Berresheim, H. (2006). Strong correlation between levels of tropospheric hydroxyl radicals and solar ultraviolet radiation. *Nature*, 442(7099), 184–187. <https://doi.org/10.1038/nature04924>
- Savarino, J., Kaiser, J., Morin, S., Sigman, D. M., & Thiemens, M. (2007). Nitrogen and oxygen isotopic constraints on the origin of atmospheric nitrate in coastal Antarctica. *Atmospheric Chemistry and Physics*, 7(8), 1925–1945. <https://doi.org/10.5194/acp-7-1925-2007>
- Savarino, J., Morin, S., Erbland, J., Grannec, F., Patey, M. D., Vicars, W., et al. (2013). Isotopic composition of atmospheric nitrate in a tropical marine boundary layer. *Proceedings of the National Academy of Sciences of the United States of America*, 110(44), 17668–17673. <https://doi.org/10.1073/pnas.1216639110>
- Shi, Y., Li, C., Jin, Z., Zhang, Y., Xiao, J., & Li, F. (2021). Combining dual isotopes and a Bayesian isotope mixing model to quantify the nitrate sources of precipitation in Ningbo, East China. *Science of the Total Environment*, 778, 146297. <https://doi.org/10.1016/j.scitotenv.2021.146297>
- Su, C., Kang, R., Zhu, W., Huang, W., Song, L., Wang, A., et al. (2020). δ¹⁵N of nitric oxide produced under aerobic or anaerobic conditions from seven soils and their associated N isotopic fractionations. *Journal of Geophysical Research: Biogeosciences*, 125, e2020JG005705. <https://doi.org/10.1029/2020JG005705>
- Sun, Y., Du, W., Wang, Q., Zhang, Q., Chen, C., Chen, Y., et al. (2015). Real-time characterization of aerosol particle composition above the urban canopy in Beijing: Insights into the interactions between the atmospheric boundary layer and aerosol chemistry. *Environmental Science & Technology*, 49(19), 11340–11347. <https://doi.org/10.1021/acs.est.5b02373>
- Tan, Z., Rohrer, F., Lu, K., Ma, X., Bohn, B., Broch, S., et al. (2018). Wintertime photochemistry in Beijing: Observations of RO_x radical concentrations in the North China Plain during the BEST-ONE campaign. *Atmospheric Chemistry and Physics*, 18(16), 12391–12411. <https://doi.org/10.5194/acp-18-12391-2018>
- Thiemens, M. H. (1999). Mass-independent isotope effects in planetary atmospheres and the Early Solar System. *Science*, 283(5400), 341–345. <https://doi.org/10.1126/science.283.5400.341>
- Vicars, W. C., Morin, S., Savarino, J., Wagner, N. L., Erbland, J., Vince, E., et al. (2013). Spatial and diurnal variability in reactive nitrogen oxide chemistry as reflected in the isotopic composition of atmospheric nitrate: Results from the CalNex 2010 field study. *Journal of Geophysical Research: Atmospheres*, 118, 10567–10588. <https://doi.org/10.1002/jgrd.50680>
- Vicars, W. C., & Savarino, J. (2014). Quantitative constraints on the ¹⁷O-excess (Δ¹⁷O) signature of surface ozone: Ambient measurements from 50°N to 50°S using the nitrite-coated filter technique. *Geochimica et Cosmochimica Acta*, 135, 270–287. <https://doi.org/10.1016/j.gca.2014.03.023>
- Vrekoussis, M., Mihalopoulos, N., Gerasopoulos, E., Kanakidou, M., Crutzen, P. J., & Lelieveld, J. (2007). Two-years of NO₃ radical observations in the boundary layer over the Eastern Mediterranean. *Atmospheric Chemistry and Physics*, 7(2), 315–327. <https://doi.org/10.5194/acp-7-315-2007>
- Walker, H. M., Stone, D., Ingham, T., Vaughan, S., Cain, M., Jones, R. L., et al. (2015). Night-time measurements of HO_x during the RONOCO project and analysis of the sources of HO₂. *Atmospheric Chemistry and Physics*, 15(14), 8179–8200. <https://doi.org/10.5194/acp-15-8179-2015>
- Walters, W. W., & Michalski, G. (2016). Theoretical calculation of oxygen equilibrium isotopic fractionation factors involving various NO_x molecules, ·OH, and H₂O and its implications for isotope variations in atmospheric nitrate. *Geochimica et Cosmochimica Acta*, 191, 89–101. <https://doi.org/10.1016/j.gca.2016.06.039>
- Wang, H., Chen, J., & Lu, K. (2017). Development of a portable cavity-enhanced absorption spectrometer for the measurement of ambient NO₃ and N₂O₅: Experimental setup, lab characterizations, and field applications in a polluted urban environment. *Atmospheric Measurement Techniques*, 10(4), 1465–1479. <https://doi.org/10.5194/amt-10-1465-2017>
- Wang, N., Lyu, X., Deng, X., Huang, X., Jiang, F., & Ding, A. (2019a). Aggravating O₃ pollution due to NO_x emission control in eastern China. *Science of the Total Environment*, 677, 732–744. <https://doi.org/10.1016/j.scitotenv.2019.04.388>

- Wang, Y. L., Song, W., Yang, W., Sun, X. C., Tong, Y. D., Wang, X. M., et al. (2019b). Influences of atmospheric pollution on the contributions of major oxidation pathways to PM_{2.5} nitrate formation in Beijing. *Journal of Geophysical Research: Atmospheres*, *124*, 4174–4185. <https://doi.org/10.1029/2019JD030284>
- Yang, Y., & Zhao, Y. (2019). Quantification and evaluation of atmospheric pollutant emissions from open biomass burning with multiple methods: A case study for the Yangtze River Delta region, China. *Atmospheric Chemistry and Physics*, *19*(1), 327–348. <https://doi.org/10.5194/acp-19-327-2019>
- Yu, H., Cao, F., Zhang, W., Zhao, Z.-Y., & Zhang, Y. (2021). Determination of ¹⁷O anomaly in atmospheric aerosol nitrate. *Chinese Journal of Analytical Chemistry*, *49*(2), 253–262. [https://doi.org/10.1016/S1872-2040\(20\)60080-9](https://doi.org/10.1016/S1872-2040(20)60080-9)
- Yu, Z., & Elliott, E. M. (2017). Novel method for nitrogen isotopic analysis of soil-emitted nitric oxide. *Environmental Science & Technology*, *51*(11), 6268–6278. <https://doi.org/10.1021/acs.est.7b00592>
- Zhang, H., Wang, Y., Hu, J., Ying, Q., & Hu, X.-M. (2015). Relationships between meteorological parameters and criteria air pollutants in three megacities in China. *Environmental Research*, *140*, 242–254. <https://doi.org/10.1016/j.envres.2015.04.004>
- Zhang, K., Zhao, C., Fan, H., Yang, Y., & Sun, Y. (2020). Toward understanding the differences of PM_{2.5} characteristics among five China urban cities. *Asia-Pacific Journal of Atmospheric Sciences*, *56*(4), 493–502. <https://doi.org/10.1007/s13143-019-00125-w>
- Zhang, Q., Xu, J., Wang, G., Tian, W., & Jiang, H. (2008). Vehicle emission inventories projection based on dynamic emission factors: A case study of Hangzhou, China. *Atmospheric Environment*, *42*(20), 4989–5002. <https://doi.org/10.1016/j.atmosenv.2008.02.010>
- Zhang, Y.-L., & Cao, F. (2015). Fine particulate matter (PM_{2.5}) in China at a city level. *Scientific Reports*, *5*(1), 14884. <https://doi.org/10.1038/srep14884>
- Zhang, Y.-L., Zhang, W., Fan, M.-Y., Li, J., Fang, H., Cao, F., et al. (2022). A diurnal story of Δ¹⁷O(NO₃⁻) in urban Nanjing and its implication for nitrate aerosol formation. *npj Climate and Atmospheric Science*, *5*(1), 50. <https://doi.org/10.1038/s41612-022-00273-3>
- Zhao, Z.-Y., Cao, F., Fan, M.-Y., Zhai, X.-Y., Yu, H.-R., Hong, Y., et al. (2021). Nitrate aerosol geochemistry and source assessment in winter at different regions in Northeast China. *Atmospheric Environment*, *267*, 118767. <https://doi.org/10.1016/j.atmosenv.2021.118767>
- Zhao, Z.-Y., Cao, F., Zhang, W.-Q., Zhai, X.-Y., Fang, Y., Fan, M.-Y., & Zhang, Y. L. (2019). Determination of stable nitrogen and oxygen isotope ratios in atmospheric aerosol nitrates. *Chinese Journal of Analytical Chemistry*, *47*(6), 907–915. [https://doi.org/10.1016/S1872-2040\(19\)61166-7](https://doi.org/10.1016/S1872-2040(19)61166-7)
- Zheng, B., Tong, D., Li, M., Liu, F., Hong, C., Geng, G., et al. (2018). Trends in China's anthropogenic emissions since 2010 as the consequence of clean air actions. *Atmospheric Chemistry and Physics*, *18*(19), 14095–14111. <https://doi.org/10.5194/acp-18-14095-2018>
- Zheng, B., Zhang, Q., Zhang, Y., He, K. B., Wang, K., Zheng, G. J., et al. (2015). Heterogeneous chemistry: A mechanism missing in current models to explain secondary inorganic aerosol formation during the January 2013 haze episode in north China. *Atmospheric Chemistry and Physics*, *15*(4), 2031–2049. <https://doi.org/10.5194/acp-15-2031-2015>
- Zong, Z., Shi, X., Sun, Z., Tian, C., Li, J., Fang, Y., et al. (2022). Nitrogen isotopic composition of NO_x from residential biomass burning and coal combustion in North China. *Environmental Pollution*, *304*, 119238. <https://doi.org/10.1016/j.envpol.2022.119238>
- Zong, Z., Tan, Y., Wang, X., Tian, C., Li, J., Fang, Y., et al. (2020). Dual-modelling-based source apportionment of NO_x in five Chinese megacities: Providing the isotopic footprint from 2013 to 2014. *Environment International*, *137*, 105592. <https://doi.org/10.1016/j.envint.2020.105592>

References From the Supporting Information

- Aneja, V. P., Nelson, D. R., Roelle, P. A., Walker, J. T., & Battye, W. (2003). Agricultural ammonia emissions and ammonium concentrations associated with aerosols and precipitation in the southeast United States. *Journal of Geophysical Research*, *108*(D4), 4152. <https://doi.org/10.1029/2002JD002271>
- Bian, Y. X., Zhao, C. S., Ma, N., Chen, J., & Xu, W. Y. (2014). A study of aerosol liquid water content based on hygroscopicity measurements at high relative humidity in the North China Plain. *Atmospheric Chemistry and Physics*, *14*(12), 6417–6426. <https://doi.org/10.5194/acp-14-6417-2014>
- Chai, J., Miller, D. J., Scheuer, E., Dibb, J., Selimovic, V., Yokelson, R., et al. (2019). Isotopic characterization of nitrogen oxides (NO_x), nitrous acid (HONO), and nitrate (pNO₃⁻) from laboratory biomass burning during FIREX. *Atmospheric Measurement Techniques*, *12*(12), 6303–6317. <https://doi.org/10.5194/amt-12-6303-2019>
- DeMore, W. B., Margitan, J., Molina, M., Watson, R., Golden, D., Hampson, R., et al. (1985). Tables of rate constants extracted from chemical kinetics and photochemical data for use in stratospheric modeling. Evaluation number 7. *International Journal of Chemical Kinetics*, *17*(10), 1135–1151. <https://doi.org/10.1002/kin.550171010>
- Jacobs, M. I., Burke, W. J., & Elrod, M. J. (2014). Kinetics of the reactions of isoprene-derived hydroxynitrates: Gas phase epoxide formation and solution phase hydrolysis. *Atmospheric Chemistry and Physics*, *14*(17), 8933–8946. <https://doi.org/10.5194/acp-14-8933-2014>
- Lee, B. H., Lopez-Hilfiker, F. D., Schroder, J. C., Campuzano-Jost, P., Jimenez, J. L., McDuffie, E. E., et al. (2018). Airborne observations of reactive inorganic chlorine and bromine species in the exhaust of coal-fired power plants. *Journal of Geophysical Research: Atmospheres*, *123*, 11225–11237. <https://doi.org/10.1029/2018JD029284>
- Li, K., Chen, L., Ying, F., White, S. J., Jang, C., Wu, X., et al. (2017). Meteorological and chemical impacts on ozone formation: A case study in Hangzhou, China. *Atmospheric Research*, *196*, 40–52. <https://doi.org/10.1016/j.atmosres.2017.06.003>
- Li, M., Zhang, Q., Kurokawa, J. I., Woo, J. H., He, K., Lu, Z., et al. (2017). MIX: A mosaic Asian anthropogenic emission inventory under the international collaboration framework of the MICS-Asia and HTAP. *Atmospheric Chemistry and Physics*, *17*(2), 935–963. <https://doi.org/10.5194/acp-17-935-2017>
- Lobert, J. M., Keene, W. C., Logan, J. A., & Yevich, R. (1999). Global chlorine emissions from biomass burning: Reactive chlorine emissions inventory. *Journal of Geophysical Research*, *104*(D7), 8373–8389. <https://doi.org/10.1029/1998JD100077>
- Michalski, G., Bhattacharya, S. K., & Girsch, G. (2014). NO_x cycle and the tropospheric ozone isotope anomaly: An experimental investigation. *Atmospheric Chemistry and Physics*, *14*(10), 4935–4953. <https://doi.org/10.5194/acp-14-4935-2014>
- Miller, D. J., Wojtal, P. K., Clark, S. C., & Hastings, M. G. (2017). Vehicle NO_x emission plume isotopic signatures: Spatial variability across the eastern United States. *Journal of Geophysical Research: Atmospheres*, *122*, 4698–4717. <https://doi.org/10.1002/2016JD025877>
- Ohura, T., Amagai, T., Shen, X., Li, S., Zhang, P., & Zhu, L. (2009). Comparative study on indoor air quality in Japan and China: Characteristics of residential indoor and outdoor VOCs. *Atmospheric Environment*, *43*(40), 6352–6359. <https://doi.org/10.1016/j.atmosenv.2009.09.022>
- Parnell, A. C., Inger, R., Bearhop, S., & Jackson, A. L. (2010). Source partitioning using stable isotopes: Coping with too much variation. *PLoS One*, *5*(3), e9672. <https://doi.org/10.1371/journal.pone.0009672>
- Ren, Y. A., Shen, G., Shen, H., Zhong, Q., Xu, H., Meng, W., et al. (2021). Contributions of biomass burning to global and regional SO₂ emissions. *Atmospheric Research*, *260*, 105709. <https://doi.org/10.1016/j.atmosres.2021.105709>

- Rindelaub, J. D., McAvey, K. M., & Shepson, P. B. (2015). The photochemical production of organic nitrates from α -pinene and loss via acid-dependent particle phase hydrolysis. *Atmospheric Environment*, *100*, 193–201. <https://doi.org/10.1016/j.atmosenv.2014.11.010>
- Sander, S., Golden, D., Kurylo, M., Moortgat, G., Wine, P., Ravishankara, A., et al. (2006). *Chemical kinetics and photochemical data for use in atmospheric studies evaluation number 15*. Jet Propulsion Laboratory, National Aeronautics and Space. Retrieved from <http://hdl.handle.net/2014/41648>
- Sharma, H. D., Jervis, R. E., & Wong, K. Y. (1970). Isotopic exchange reactions in nitrogen oxides. *The Journal of Physical Chemistry*, *74*(4), 923–933. <https://doi.org/10.1021/j100699a044>
- Shi, Y., Tian, P., Jin, Z., Hu, Y., Zhang, Y., & Li, F. (2022). Stable nitrogen isotope composition of NO_x of biomass burning in China. *Science of the Total Environment*, *803*, 149857. <https://doi.org/10.1016/j.scitotenv.2021.149857>
- Stevens, R. G., Pierce, J. R., Brock, C. A., Reed, M. K., Crawford, J. H., Holloway, J. S., et al. (2012). Nucleation and growth of sulfate aerosol in coal-fired power plant plumes: Sensitivity to background aerosol and meteorology. *Atmospheric Chemistry and Physics*, *12*(1), 189–206. <https://doi.org/10.5194/acp-12-189-2012>
- Walters, W. W., Goodwin, S. R., & Michalski, G. (2015). Nitrogen stable isotope composition ($\delta^{15}\text{N}$) of vehicle-emitted NO_x . *Environmental Science & Technology*, *49*(4), 2278–2285. <https://doi.org/10.1021/es505580v>
- Walters, W. W., Tharp, B. D., Fang, H., Kozak, B. J., & Michalski, G. (2015). Nitrogen isotope composition of thermally produced NO_x from various fossil-fuel combustion sources. *Environmental Science & Technology*, *49*(19), 11363–11371. <https://doi.org/10.1021/acs.est.5b02769>
- Wang, Q., Li, S., Dong, M., Li, W., Gao, X., Ye, R., & Zhang, D. (2018). VOCs emission characteristics and priority control analysis based on VOCs emission inventories and ozone formation potentials in Zhoushan. *Atmospheric Environment*, *182*, 234–241. <https://doi.org/10.1016/j.atmosenv.2018.03.034>
- Wang, X., Zhang, Y., Chen, H., Yang, X., Chen, J., & Geng, F. (2009). Particulate nitrate formation in a highly polluted urban area: A case study by single-particle mass spectrometry in Shanghai. *Environmental Science & Technology*, *43*(9), 3061–3066. <https://doi.org/10.1021/es8020155>
- Xu, L., Guo, H., Boyd, C. M., Klein, M., Bougiatioti, A., Cerully, K. M., et al. (2015). Effects of anthropogenic emissions on aerosol formation from isoprene and monoterpenes in the southeastern United States. *Proceedings of the National Academy of Sciences of the United States of America*, *112*(1), 37–42. <https://doi.org/10.1073/pnas.1417609112>
- Zaveri, R. A., Berkowitz, C. M., Brechtel, F. J., Gilles, M. K., Hubbe, J. M., Jayne, J. T., et al. (2010). Nighttime chemical evolution of aerosol and trace gases in a power plant plume: Implications for secondary organic nitrate and organosulfate aerosol formation, NO_3 radical chemistry, and N_2O_5 heterogeneous hydrolysis. *Journal of Geophysical Research*, *115*, D12304. <https://doi.org/10.1029/2009JD013250>